MODELING STRESS CONCENTRATION EFFECTS IN COMPOSITE PLATES

Lucas L. Vignoli[1,2]*, Jaime T. P. Castro[1], Marco A. Meggiolaro[1]

[1]Department of Mechanical Engineering, Pontifical Catholic University of Rio de Janeiro, Rio de Janeiro, RJ, Brazil

[2]Department of Mechanical Engineering, COPPE/UFRJ, Federal University of Rio de Janeiro, Rio de Janeiro, RJ, Brazil

*Corresponding author: lucaslvig@gmail.com

Abstract: Holes generate localized concentration effects on stresses and strains fields, but they are usually unavoidable in real structures for functional reasons. This paper studies such effects induced by circular holes in composite plates under several load conditions. First the Stroh Formalism is introduced and used to obtain the elastic stress solution on the border of these holes subjected to general in-plane loads, and then Tsai-Wu's, Puck's, and LaRC05 failure models are applied to predict the initial damage using the First-Ply-Failure (FPF) methodology. These theories were chosen because they performed well on the World Wide Failure Exercise (WWFE) and properly address the macromechanics of the stress concentration problem. Just single layered unidirectional laminates are evaluated, but the methodology can be extended for any laminate. The main differences between FPF predictions occur when the fibers fail under compression, since the hypotheses used for Puck and LaRC05 models in such cases are completely different. The difference between initial damage predictions considering plane stress and plane strain limit conditions may also be significant, depending on the failure criteria and load conditions.

Keywords: Stress Concentration, Stroh Formalism, Laminate composite plates.

1. INTRODUCTION

Even though notches locally concentrate stresses and strains, they are needed in most structures for functional reasons, so they usually are unavoidable in practice. For isotropic materials, this topic had already been exhaustively studied [1], but for anisotropic materials the few solutions available were obtained with the Lekhniskii formalism [2], although the newer Stroh formalism has several advantages over it for plane (stress or strain) elasticity [3,4]. So, this simpler method is used in this paper to obtain the stress distribution along the border of a circular hole in a large composite plate subjected to general in-plane loads. Moreover, to estimate the damage around the hole, Tsai-Wu, Puck, and LaRC05 failure criteria are applied using the damage-free design methodology, as recommended by the World Wide Failure Exercise (WWFE) [5,6]. However, since none of them generated systematically better previsions in all tests, the WWFE concluded that it is still necessary to compare theirs estimates, a procedure used in this work as well.

Using the Stroh formalism and the WWFE recommendations, different load conditions are studied to evaluate the influence of fibers inclination in a single layered unidirectional laminate. Since just initial damage is analyzed in this paper, notice that its progression is not evaluated. But the effect of

the plate thickness in the failure mechanism is considered using the plane strain assumption. For any finite plate thickness it is expected that the actual stresses lie between the two considered bounds, plane stress and plane strain conditions. The materials properties used in these analyses are listed in Table 1. The difference between plane stress and plane strain strength estimates can be larger than 60%, indicating that further investigation of the thickness influence is recommended. The main difference between the failure models used here is how they treat fiber failure under compression. The LaRC05 criterion assumes damage considerable before the others, since it considers fiber instability.

Table 1: Mechanical properties of carbon/epoxy used in this work [7]

Elastic Properties		Strengths	
E_1	140 GPa	S_{11}^t	1990 MPa
$E_2 = E_3$	10 GPa	S_{11}^c	1500 MPa
$G_{12} = G_{13}$	6 GPa	$S_{22}^t = S_{33}^t$	38 MPa
G_{23}	3.35 GPa	$S_{22}^c = S_{33}^c$	150 MPa
$\nu_{12} = \nu_{13}$	0.3	$S_{12} = S_{13}$	70 MPa
ν_{23}	0.49	S_{23}	50 MPa
$E_1^{(f)}$	231 GPa		
$\nu_{12}^{(f)}$	0.2		

2. STROH FORMALISM

The Stroh formalism is a powerful mathematical tool to model anisotropic elasticity, which has been successfully used to solve several 2D problems, see Ting [3] and Hwu [4] for further details.

In a general way, the equilibrium requirements, geometrical compatibility, and linear elastic constitutive relations are expressed as

$$\sigma_{ij,j} = 0 \tag{1}$$

$$\varepsilon_{ij} = \frac{1}{2}(u_{i,j} + u_{j,i}) \tag{2}$$

$$\sigma_{ij} = s_{ijkl}\varepsilon_{kl} \tag{3}$$

To start with, suppose a displacement field solution with the form $u_k = v_k f(z)$, where v_k depends on material constants (eigenvector) and $f(z)$ is a generic function that depends on the boundary conditions and also on material properties. Considering, without loss of generality, $z = x_1 + px_2$, where p is a material constant (eigenvalue), it can be shown that

$$\left[Q_{ik} + (R_{ik} + R_{ki})p + T_{ik}p^2\right]v_k = 0 \tag{4}$$

where $Q_{ik} = s_{i1k1}$, $R_{ik} = s_{i1k2}$ and $T_{ik} = s_{i2k2}$.

However, these equations consider that the reference coordinate system coincides with the material coordinates, but this is not necessarily true in practical applications, and usually it is not. In fact, to obtain the stress distribution around a circular hole in a large anisotropic plate it is necessary to use three coordinate systems; one to define the load, called global in this paper; another to define the material properties, named material coordinates; and the last one to map the hole border. To use a

clear notation, an upper index is used to reference the global and local coordinates. The following relations are helpful to relate these coordinates:

$$\mathbf{Q}^{(l)} = \mathbf{Q}\cos^2\theta + \left(\mathbf{R} + \mathbf{R}^T\right)\sin\theta\cos\theta + \mathbf{T}\sin^2\theta \tag{5}$$

$$\mathbf{R}^{(l)} = \mathbf{R}\cos^2\theta + \left(\mathbf{T} - \mathbf{Q}\right)\sin\theta\cos\theta + \mathbf{R}^T\sin^2\theta \tag{6}$$

$$\mathbf{T}^{(l)} = \mathbf{T}\cos^2\theta - \left(\mathbf{R} + \mathbf{R}^T\right)\sin\theta\cos\theta + \mathbf{Q}\sin^2\theta \tag{7}$$

Using the Airy stress function, considering a solution of the form $\phi_i = w_i f(z)$ and satisfying the boundary condition $\phi\big|_\infty \to \phi^\infty$ and $\phi\big|_\Gamma = 0$, and using the conformal mapping technique, the stress solution can be expressed as

$$\sigma_{11}^{(l)} = \mathbf{i_1}\left(\mathbf{G}_1^{(l)}\boldsymbol{\tau}_2 + \mathbf{G}_3^{(l)}\boldsymbol{\tau}_1\right) - \mathbf{i}_2\left(\mathbf{G}_1^{(l)}\boldsymbol{\tau}_1 - \mathbf{G}_3^{(l)}\boldsymbol{\tau}_2\right) \tag{8}$$

were $\mathbf{i_1} = \begin{bmatrix}1 & 0 & 0\end{bmatrix}$, $\mathbf{i}_2 = \begin{bmatrix}0 & 1 & 0\end{bmatrix}$, $\mathbf{G}_1^{(l)} = \left[\mathbf{N}_1^{(l)}\right]^T - \mathbf{N}_3^{(l)}\mathbf{S}\mathbf{L}^{-1}$, $\mathbf{G}_3^{(l)} = -\mathbf{N}_3^{(l)}\mathbf{L}^{-1}$, $\boldsymbol{\tau}_1 = \begin{bmatrix}\sigma_{11} & \sigma_{12} & 0\end{bmatrix}^T$ and $\boldsymbol{\tau}_2 = \begin{bmatrix}\sigma_{21} & \sigma_{22} & 0\end{bmatrix}^T$. The components of the fundamental matrix of elasticity are

$$\mathbf{N}_1^{(l)} = -\left[\mathbf{T}^{(l)}\right]^{-1}\left[\mathbf{R}^{(l)}\right]^T \tag{9}$$

$$\mathbf{N}_3^{(l)} = -\mathbf{R}^{(l)}\left[\mathbf{T}^{(l)}\right]^{-1}\left[\mathbf{R}^{(l)}\right]^T - \mathbf{Q}^{(l)} \tag{10}$$

and the Barnet-Lothe tensors are defined for an orthotropic material as

$$\mathbf{S}_{\mathrm{BL}} = \begin{bmatrix} 0 & \left(\mathbf{S}_{\mathrm{BL}}\right)_{12} & 0 \\ \left(\mathbf{S}_{\mathrm{BL}}\right)_{21} & 0 & 0 \\ 0 & 0 & 0 \end{bmatrix} \tag{11}$$

$$\mathbf{L}_{\mathrm{BL}} = \begin{bmatrix} \left(\mathbf{L}_{\mathrm{BL}}\right)_{11} & 0 & 0 \\ 0 & \left(\mathbf{L}_{\mathrm{BL}}\right)_{22} & 0 \\ 0 & 0 & \left(\mathbf{L}_{\mathrm{BL}}\right)_{33} \end{bmatrix} \tag{12}$$

where, for plane stress,

$$\left(S_{BL}\right)_{12} = \left[\left(E_2/G_{12}\right) + 2\left(1 - \sqrt{\nu_{12}\nu_{21}}\right)\sqrt{E_2/E_1}\right]^{-1/2}\left(1 - \sqrt{\nu_{12}\nu_{21}}\right) \tag{13}$$

$$\left(S_{BL}\right)_{21} = -\left\{\frac{\left(\frac{E_1}{G_{12}}\right) + 2\left(1 - \sqrt{\nu_{12}\nu_{21}}\right)\sqrt{\frac{E_1}{E_2}}}{\left(\frac{E_2}{G_{12}}\right) + 2\left(1 - \sqrt{\nu_{12}\nu_{21}}\right)\sqrt{\frac{E_2}{E_1}}}\left[\left(\frac{E_2}{G_{12}}\right) + 2\left(1 - \sqrt{\nu_{12}\nu_{21}}\right)\sqrt{\frac{E_2}{E_1}}\right]\right\}^{-\frac{1}{2}}\left(1 - \sqrt{\nu_{12}\nu_{21}}\right) \tag{14}$$

$$\left(L_{BL}\right)_{11} = \left[E_1/\left(1 - \sqrt{\nu_{12}\nu_{21}}\right)\right]\left[\left(E_2/G_{12}\right) + 2\left(1 - \sqrt{\nu_{12}\nu_{21}}\right)\sqrt{E_2/E_1}\right]^{-1/2}\left(1 - \sqrt{\nu_{12}\nu_{21}}\right) \tag{15}$$

$$\left(L_{BL}\right)_{22} = -\left[\frac{E_1}{\left(1-\sqrt{\nu_{12}\nu_{21}}\right)}\right]\left\{\frac{\left(\frac{E_1}{G_{12}}\right)+2\left(1-\sqrt{\nu_{12}\nu_{21}}\right)\sqrt{\frac{E_1}{E_2}}}{\left(\frac{E_2}{G_{12}}\right)+2\left(1-\sqrt{\nu_{12}\nu_{21}}\right)\sqrt{\frac{E_2}{E_1}}}\left[\left(\frac{E_2}{G_{12}}\right)+2\left(1-\sqrt{\nu_{12}\nu_{21}}\right)\sqrt{\frac{E_2}{E_1}}\right]\right\}^{-\frac{1}{2}}\left(1-\sqrt{\nu_{12}\nu_{21}}\right) \tag{16}$$

$$\left(L_{BL}\right)_{33} = \sqrt{G_{13}G_{23}} \tag{17}$$

3. FAILURE CRITERIA

This section briefly introduces the failure criteria used here. Additional details are found in references [8] for Tsai-Wu, [9] for Puck, and [10] for LaRC05.

3.1 Tsai-Wu

Tsai-Wu model is the most popular of those used in this paper. It has an adjustable polynomial function and can be expressed as

$$\begin{aligned} f_{TW} = {} & \frac{\sigma_{11}^2}{S_{11}^t S_{11}^c} + \frac{\left(\sigma_{22}^2+\sigma_{33}^2\right)}{S_{22}^t S_{22}^c} + \frac{\sigma_{12}^2+\sigma_{13}^2}{\left(S_{12}\right)^2} + \left(\frac{\sigma_{23}}{S_{23}}\right)^2 + a_{12}\sigma_{11}\left(\sigma_{22}+\sigma_{33}\right) + \\ & + a_{23}\sigma_{22}\sigma_{33} + \left(\frac{1}{S_{11}^t}-\frac{1}{S_{11}^c}\right)\sigma_{11} + \left(\frac{1}{S_{22}^t}-\frac{1}{S_{22}^c}\right)\left(\sigma_{22}+\sigma_{33}\right) \end{aligned} \tag{18}$$

Despite no phenomenological basis, it has a great advantage of easer applicability.

3.2 Puck

Puck model use the following four different equations to model fiber and matrix failure under tension and compression

$$f_P^{(f,t)} = \left(1/S_{11}^t\right)\cdot\left|\sigma_{11} + \left[\left(E_1/E_1^{(f)}\right)\nu_{12}^{(f)}m_f - \nu_{12}\right]\left(\sigma_{22}+\sigma_{33}\right)\right| \tag{19}$$

$$f_P^{(f,c)} = \left(1/S_{11}^c\right)\cdot\left|\sigma_{11} + \left[\left(E_1/E_1^{(f)}\right)\nu_{12}^{(f)}m_f - \nu_{12}\right]\left(\sigma_{22}+\sigma_{33}\right)\right| + \left(10\,\sigma_{12}/G_{12}\right)^2 \tag{20}$$

$$f_P^{(m,c)} = \left(\sigma_{12}^{\Phi}/S_{12}^{\Phi}\right)^2 + 2\left(p_{\Phi}^c/S_{12}^{\Phi}\right)\sigma_{22}^{(23)} + \left(\sigma_{11}/X_{11}\right)^n \tag{21}$$

$$f_P^{(m,t)} = \left(\sigma_{12}^{\Phi}/S_{12}^{\Phi}\right)^2 + 2\left(p_{\Phi}^t/S_{12}^{\Phi}\right)\sigma_{22}^{(23)} + \left(1-2p_{\Phi}^t\,S_{22}^t/S_{12}^{\Phi}\right)\left(\sigma_{22}^{(23)}/S_{22}^t\right)^2 + \left(\sigma_{11}/X_{11}\right)^n \tag{22}$$

where m_f is equal to 1.3 for carbon fiber in polymeric matrix, $X_{11} = 1.1S_{11}^t$ if $\sigma_{11} \geq 0$ or $X_{11} = -1.1S_{11}^c$ if $\sigma_{11} < 0$ and $6 \leq n \leq 8$. The stress components on the critical plane are computed as $\sigma_{ij}^{(23)} = \lambda_{ik}\lambda_{jl}\sigma_{kl}$, where $\lambda_{ij} = \cos\left(x_i, x_j\right)$ and the angle between x_2 and $x_2^{(23)}$ is γ. At last to quantify the shear effect, the "equivalent" shear is calculated as $\sigma_{12}^{\Phi} = \sqrt{\left[(\sigma_{12}^{(23)})^2 + (\sigma_{23}^{(23)})^2\right]}$ and assuming p_{12}^c and p_{12}^t are equal respectivly to 0.3 and 0.35 for carbon fiber, the quantities $\left(\sigma_{12}^{\Phi}/S_{12}^{\Phi}\right)^2 = \left(\sigma_{12}^{(23)}/S_{12}\right)^2 + \left(\sigma_{23}^{(23)}/S_{23}^{(23)}\right)^2$, $p_{\Phi}^c = S_{12}^{\Phi}\left(p_{12}^c/S_{12}\right)$, $p_{\Phi}^t = S_{12}^{\Phi}\left(p_{12}^t/S_{12}\right)$, $S_{23}^{(23)} = \left(S_{12}/2p_{12}^c\right)\cdot\left[\sqrt{\left(1+2p_{12}^c\,S_{22}^c/S_{12}\right)}-1\right]$ can be calculated.

3.3 LaRC05

LaRC05 models also propose different models for fibers under tension or compression, using just an additional term to calculate the matrix damage under tension. These equations are

$$f_L^{(f,t)} = \sigma_{11} \big/ S_{11}^t \tag{23}$$

$$f_L^{(f,c)} = \left[\sigma_{12}^{(mis)} \Big/ \left(S_{12} - b_L \sigma_{22}^{(mis)}\right)\right]^2 + \left[\sigma_{23}^{(mis)} \Big/ \left(S_{23}^{(mis)} - b_T \sigma_{22}^{(mis)}\right)\right]^2 + \left[\max\left\{0, \sigma_{22}^{(23)}\right\} \Big/ S_{22}^t\right]^2 \tag{24}$$

$$f_L^{(m)} = \left[\sigma_{12}^{(23)} \Big/ \left(S_{12} - b_L \sigma_{22}^{(23)}\right)\right]^2 + \left[\sigma_{23}^{(23)} \Big/ \left(S_{23}^{(23)} - b_T \sigma_{22}^{(23)}\right)\right]^2 + \left[\max\left\{0, \sigma_{22}^{(23)}\right\} \Big/ S_{22}^t\right]^2 \tag{25}$$

A stress decomposition similar to Puck's model is necessary to obtain the critical plane, using $b_T = -\left(1/\tan 2\theta_0\right)$, $S_{23}^{(23)} = S_{22}^c \cos\theta_0 \left(\sin\theta_0 + \cos\theta_0 / \tan 2\theta_0\right)$, $b_L = 0.082$ and $\theta_0 = 53°$. However, for fiber under compression and completely different approach is proposed here.

Two stress component decompositions are needed; first to find the critical plane $\sigma_{ij}^{(\phi)} = \lambda_{ik}\lambda_{jl}\sigma_{kl}$, where ϕ is the angle between $x_2^{(\phi)}$ and x_2, and then $\sigma_{ij}^{(mis)} = \lambda_{ik}\lambda_{jl}\sigma_{kl}^{(\phi)}$ to obtain the stress components on the fiber misalignment direction of the critical plane. The initial misalignment angle is $\varphi_0 = \left(1 - S_{11}^c / G_{12}\right) a \tan\left[\left(1 - \sqrt{1 - 4\left(S_{12}/S_{11}^c + b_L\right) S_{12}/S_{11}^c}\right) \Big/ 2\left(S_{12}/S_{11}^c + b_L\right)\right]$, a material property.

4. RESULTS AND DISCUSSION

Strength is associated with initial damage and the index FPF (First-Ply Failure) clarifies this in the notation. Due to space limits, just uniaxial loads are discussed following, but additional results are available in [12]. To start with, Fig. 1 shows the stress components distributions around the circular hole border in material coordinates, for a range of fiber-to-load angles α.

Comparing with the classical results for isotropic materials, where stress concentration effects range from -1 to 3, in a single lay laminated plate such effects range from -4 to 7. Predictions of tensile and compressive FPF strengths for these cases by the three failure criteria used in this work are shown in Fig. 2, as a function of the fibers angle. For tension the failure theories yield similar results, while for compression they generate significantly different predictions. The results are normalized by the largest strength, which is on the fibers direction. Notice that according to table 1, $S_{11}^t / S_{22}^t = 52.4$ and $S_{11}^c / S_{22}^c = 10$, so matrix failure tends to be the dominant mechanism in Fig. 2.

For tensile loads, when $\alpha = 0°$, it is expected that damage initiates for $90MPa < \sigma_{11}^{(g)} < 100MPa$ according to all models and for compressive loads, when $\alpha = 15°$ and $\sigma_{11}^{(g)} = -70MPa$, just LaRC05 model indicates failure. The models function estimations are presented in Fig. 3. Note however that contrary to what happens in isotropic plates, failure is expected in this case at $\theta \cong \mp 20°$, instead of at $\theta = 0°$ for tension and $\theta \cong 170°$ for compression. Note that the maximum stress concentration location is NOT necessarily the critical point around the hole border.

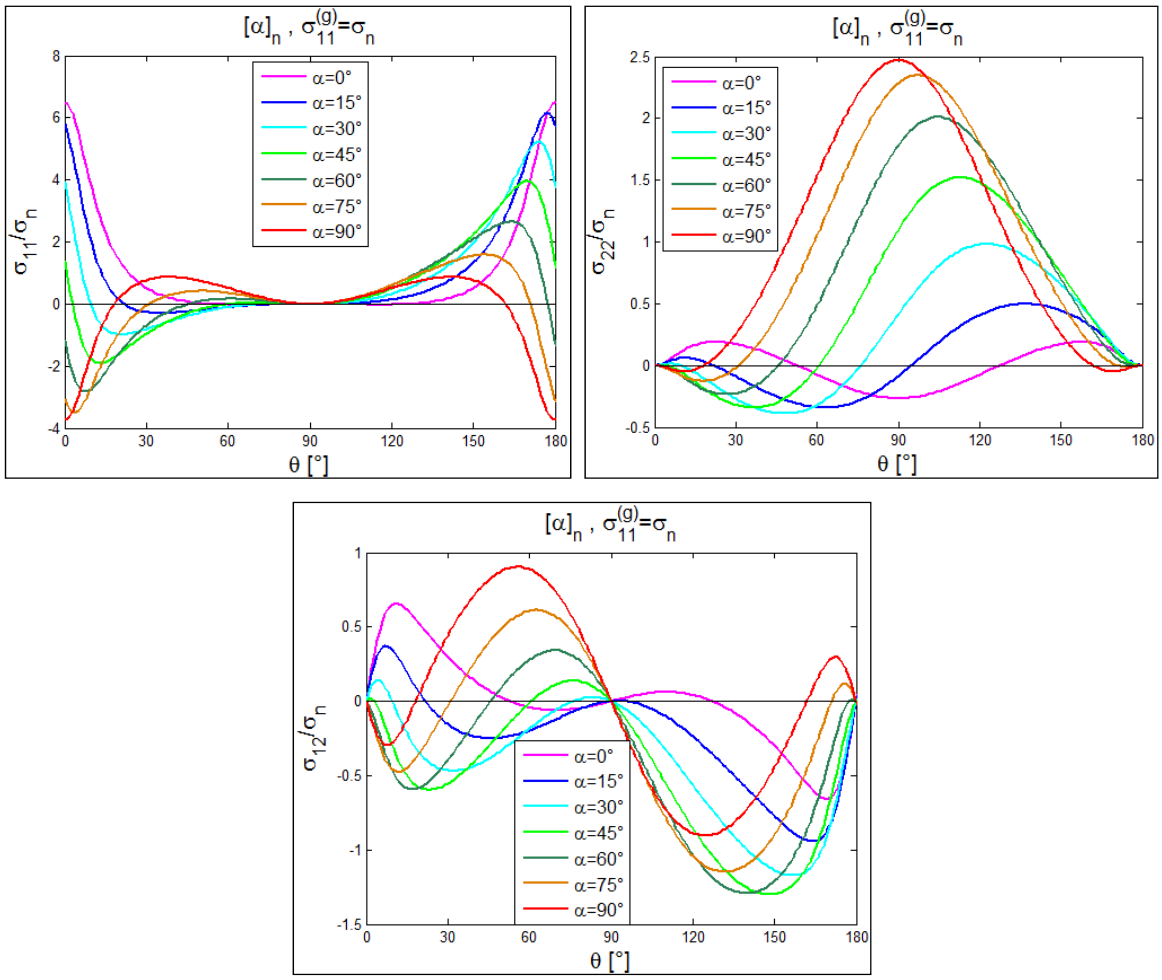

Figure 1: Stress concentration in material coordinate for a circular hole under plane stress.

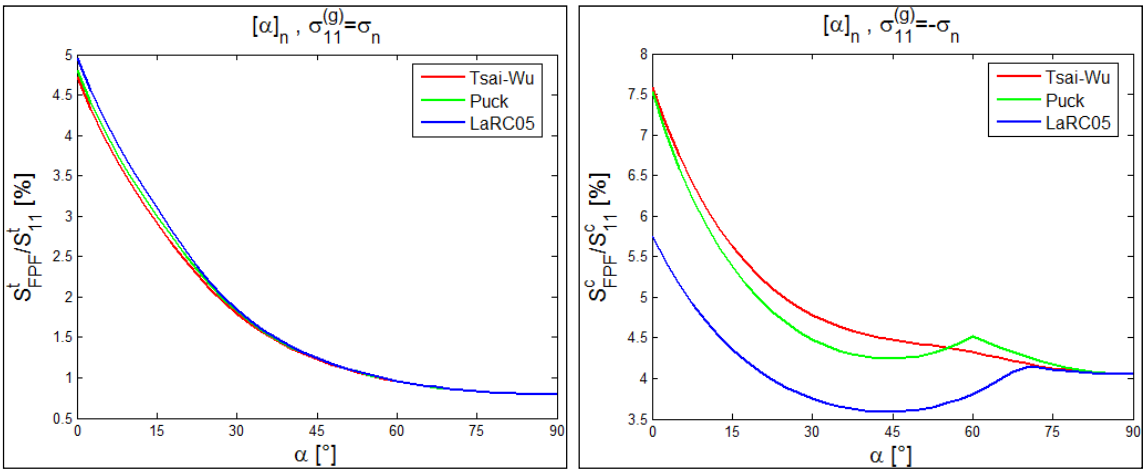

Figure 2: Normalized strength predictions for three failure criteria for uniaxial tension and compression applied to a large plate with circular hole under plane stress.

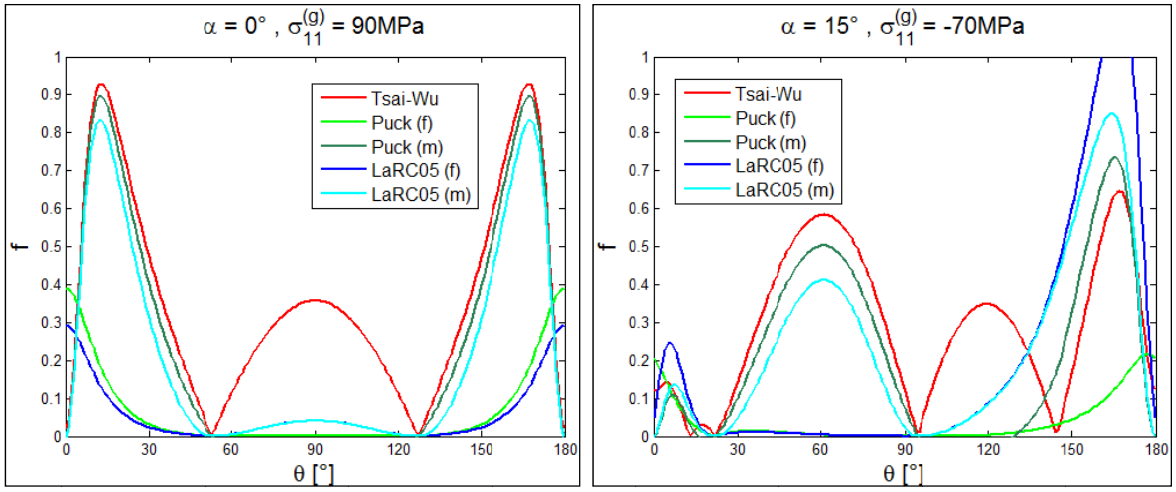

Figure 3: Critical points for tension and compression loads.

The Stroh formalism may be modified for plane strain problems. For additional discussions, see [3,4]. The stress distribution are omitted here, but the additional component (σ_{33}) can be even larger than the nominal applied stress depending of the fibers-to-load angle [11].

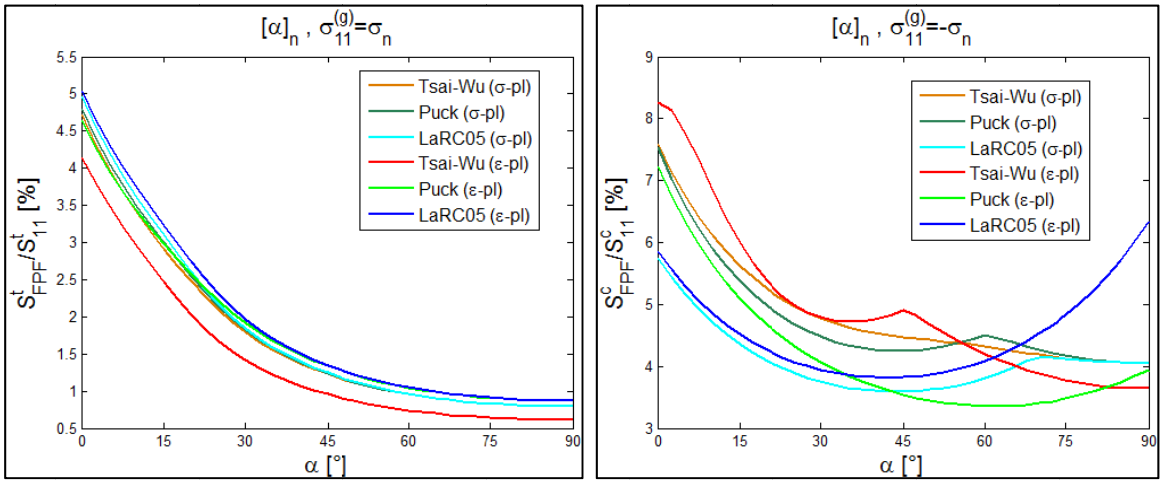

Figure 4: Comparison between normalized strength predictions for three failure criteria for uniaxial tension and compression applied to a large plate with circular hole under plane stress and plane strain.

Considering the plane strain hypothesis as an upper bound for thick plates, while plane stress is more appropriated for thin plates (lower bound) [12], the failure criteria are applied to estimate the maximum error generated on the strength estimation when the thickness effect is despised. Assuming the plane strain hypothesis the strengths were obtained following the same procedure than for plane stress and are presented in Fig. 4. To get an easier comparison, the strengths estimated for plane stress are also plotted together. For tension, the tendencies remain similar (not equal), but for compression the results are very different both on curve shape and magnitude aspects. The largest variation is for LaRC05 because the multiaxial stress state has influence in fiber instability.

5. CONCLUSIONS

Uniaxial tension and compression stress concentration effects around the border of a circular hole in a very large anisotropic plate were analyzed for plane stress and plane strain conditions. Clearly, the fibers inclination which produces the higher stress concentration do not means the critical fiber-to-load angle, as pointed out by Vignoli et al [13]. This result is basically because the higher stress component is acting on the fibers, which have a much higher strength than the matrix.

The thickness effect was evaluated and it was proved that it must be considered for design purpose because the errors generated are not disregarded for all the criteria, becomes even more significate for fiber under compression according to LaRC05 (up to 60%).

ACKNOWLEDGEMENTS

L.L. Vignoli is grateful for scholarships granted by PUC-Rio, CNPq and CAPES.

REFERENCES

[1] G.N. Savin, Stress Distribution Around Holes, NASA Technical Translation, Washington, D.C., 1970.

[2] S.G. Lekhniskii, Anisotropic Plates, third ed., Gordon and Breach Science Publishers, New York, 1987.

[3] T.C.T. Ting, 1996. Anisotropic Elasticity: Theory and Applications, Oxford University Press, 1996.

[4] C. Hwu, Anisotropic Elastic Plates. Springer, 2009.

[5] P.D. Soden, A.S. Kaddour, M.J. Hinton, Recommendations for designers and researchers resulting from the world-wide failure exercise, Compos. Sci. Technol. **64**, pp. 589–604, 2004.

[6] A.S. Kaddour, M.J. Hinton, Maturity of 3D failure criteria for fibre reinforced composites: Comparison between theories and experiments: Part B of WWFE-II, J. Compos. Mater. **47**, pp. 925–966, 2013.

[7] M.J. Hinton, A.S. Kaddour, and P.D. Soden (Editors), Failure Criteria in Fibre Reinforced Polymer Composites: The World-Wide Failure Exercise, Elsevier, 2004.

[8] K.S. Liu, S.W. Tsai, A progressive quadratic failure criterion for a laminate, Compos. Sci. Technol. **58**, pp. 1023-1032, 1998.

[9] A. Puck, H. Schürmann, Failure analysis of FRP laminates by means of physically based phenomenological models, Compos. Sci. Technol. **58**, pp. 1045-1067, 1998.

[10] S.T. Pinho, R. Darvizeh, P. Robinson, C. Schuecker, P.P. Camanho, Material and structural response of polymer-matrix fibre-reinforced composites, J. Compos. Mater. **46**, pp.2313-2341, 2012.

[11] L.L. Vignoli, An Study of Stress Concentration Effects in Anisotropic Materials Applied to Unidirectional Laminate Composites (in Portuguese), M.Sc. Thesis, PUC-Rio, Rio de Janeiro, 2016.

[12] R.C.O. Góes, J. T. P. Castro, L. F. Martha. 3D effects around notch and crack tips. Int. J. Fatigue **62**, pp.159-170, 2014.

[13] L.L. Vignoli, J.T.P. Castro, M.A. Meggiolaro, Stress Concentration Analysis in Orthotropic Plates, *Proceedings of the 23rd ABCM International Congress of Mechanical Engineering – COBEM*, Rio de Janeiro, pp.1-8, 2015.